processes

MDPI

Article

The Influence of Mg, Na, and Li Oxides on the CO_2 Sorption Properties of Natural Zeolite

Manshuk Mambetova [1,2,*], Kusman Dossumov [1] and Gaukhar Yergaziyeva [1,2]

[1] Center of Physical Chemical Methods of Research and Analysis, Al-Farabi Kazakh National University, Tole Bi str. 96A, Almaty 050012, Kazakhstan; ergazieva_g@mail.ru (G.Y.)
[2] The Laboratory of Catalytic Processes, Institute of Combustion Problems, Bogenbay Batyr Str. 172, Almaty 050012, Kazakhstan
* Correspondence: mambetova_manshuk@list.ru; Tel.: +7-747-402-40-52

Abstract: This study presents a comparative analysis of the CO_2 sorption properties of natural zeolites sourced from the Tayzhuzgen (Tg) and Shankanay (Sh) deposits in Kazakhstan. The Tayzhuzgen zeolite was characterized by a Si/Al ratio of 5.6, suggesting partial dealumination, and demonstrated enhanced specific surface area following mechanical activation. Modification of the Tayzhuzgen zeolite with magnesium oxide significantly improved its CO_2 sorption capacity, reaching 8.46 mmol CO_2/g, attributed to the formation of the $CaMg(Si_2O_6)$ phase and the resulting increase in basic active sites. TPD-CO_2 analysis confirmed that MgO/Tg exhibited the highest basicity of the modified samples, further validating its potential for CO_2 capture applications.

Keywords: natural zeolites; sorbents; carbon dioxide; CO_2 capture; adsorption capacity

1. Introduction

Carbon dioxide (CO_2) is a primary greenhouse gas contributing significantly to climate change, with emissions primarily resulting from industrial activities and fossil fuel combustion [1,2]. The urgent need to mitigate CO_2 emissions has driven intensive research into carbon capture and storage (CCS) technologies, which aim to capture CO_2 directly from industrial sources and prevent its release into the atmosphere [3]. Several methodologies are currently employed for CO_2 capture, each with distinct advantages and challenges.

One of the most common approaches is chemical absorption, where CO_2 is absorbed into solvents, such as amines, which form chemical bonds with the gas [4]. This method is widely used in industry due to its high efficiency, but it is energy-intensive, particularly during the regeneration process of the solvent. Physical absorption, another method, utilizes non-reactive solvents like methanol to dissolve CO_2 under high pressure. However, this approach is effective only under specific conditions, such as low temperatures and high CO_2 concentrations, limiting its broader application [5].

Adsorption methods, which rely on solid sorbents, are gaining attention due to their lower energy demands and potential for regeneration [6]. Among these, solid adsorbents such as zeolites, metal–organic frameworks (MOFs), and activated carbons offer high CO_2 selectivity and adsorption capacities, especially at elevated temperatures [7]. The primary limitation with synthetic adsorbents, however, lies in their high cost and complex synthesis processes, which can restrict their scalability for industrial applications. Compared to synthetic zeolites, natural zeolites offer an economical and efficient solution as they can be used directly with minimal processing [8,9].

Natural zeolites, a group of aluminosilicate minerals formed through volcanic processes, have emerged as promising candidates for CO_2 capture due to their unique physicochemical properties [9,10]. Their highly porous structure enables them to function as molecular sieves, making them ideal sorbents for capturing gasses such as CO_2. The global reserves of natural zeolites are substantial, and their use spans various industries, including

check for updates

Citation: Mambetova, M.; Dossumov, K.; Yergaziyeva, G. The Influence of Mg, Na, and Li Oxides on the CO_2 Sorption Properties of Natural Zeolite. *Processes* **2024**, *12*, 2592. https://doi.org/10.3390/pr12112592

Academic Editor: Juan García Rodríguez

Received: 10 October 2024
Revised: 8 November 2024
Accepted: 15 November 2024
Published: 18 November 2024

environmental protection, water purification, and air filtration [11]. Among the common types of zeolites are clinoptilolite, mordenite, phillipsite, and chabazite, which are classified based on their mineral content into high-grade (more than 70% zeolite), medium-grade (50–70%), and low-grade (15–50%) varieties [12].

While zeolites are widely recognized for their ability to adsorb and retain various substances, including toxic and radioactive compounds [13,14], their application in CO_2 capture, particularly under industrial conditions, remains a relatively underexplored area. In Kazakhstan, the Tayzhuzgen (with confirmed reserves of 7 million tons and estimated reserves of 215 million tons) and Shankanay (with confirmed reserves of 5.5 million tons and estimated reserves of 120 million tons) deposits represent some of the country's largest natural zeolite reserves [15,16]. These deposits hold significant promise for industrial applications due to the high quality of their zeolites, especially in the context of CO_2 capture technologies.

Research on Kazakhstan's natural zeolites has primarily focused on their ability to remove heavy metals, such as lead and cadmium, from aqueous solutions [17–20]. In addition, zeolites are used in agriculture as feed additives to improve the productivity of livestock and poultry, as well as to increase the yield of agricultural crops. However, their potential for CO_2 adsorption is yet to be comprehensively examined, presenting new research opportunities.

Given the abundance and lower cost of natural zeolites compared to synthetic alternatives, their potential in CO_2 capture has garnered increasing attention. Additionally, modifications with alkali and alkaline earth metals can further enhance the sorption properties of zeolites, making them more effective in capturing CO_2 at elevated temperatures. The aim of this study is to investigate the CO_2 capture properties of natural zeolites from the Tayzhuzgen and Shankanay deposits. While previous research has focused on the removal of heavy metals, this is the first comprehensive study exploring their CO_2 adsorption capacity. The primary objective is to assess the physicochemical properties of these zeolites and evaluate their effectiveness in capturing CO_2. The results of this study will contribute to expanding the knowledge base on natural zeolites and their environmental applications, particularly in reducing CO_2 emissions. Understanding the sorption characteristics of these materials may reveal their potential as low-cost and efficient sorbents for CO_2 capture, thereby supporting global efforts to mitigate climate change.

2. Materials and Reagents

The chemicals used in this research were of the highest purity, obtained from reliable commercial sources to ensure accuracy and consistency in the experimental procedures. Magnesium nitrate, lithium nitrate, and sodium carbonate were obtained from Sigma-Aldrich, a trusted provider of high-purity reagents. All zeolite samples were prepared using deionized water, which was employed to eliminate potential contaminants and maintain the integrity of the chemical processes. For the preparation of natural zeolite suspensions, deionized water was used to maintain stringent control over the purity of the experimental conditions. In the subsequent CO_2 adsorption experiments, gasses such as high-purity (99.99%) carbon dioxide (CO_2), argon (Ar), and helium (He) were supplied by Ihsan Technogas LLP (Almaty, Kazakhstan) ensuring accuracy in the adsorption–desorption cycles.

Sorbent Synthesis

To evaluate the CO_2 adsorption efficiency of natural zeolites from Kazakhstan, samples were collected from the Tayzhuzgen and Shankanay deposits. The initial preparation involved reducing the particle size of the zeolite samples to 0.25–0.5 mm through mechanical crushing. After sieving, the samples were mixed with deionized water to form a uniform paste, which was then molded into cylindrical pellets with a diameter and height of 2.7 mm. The prepared paste was placed in a small mold (Figure 1), allowing for the formation of uniformly shaped granules in a single technological step. The pellets

underwent controlled heating in a muffle furnace set to 600 °C for 5 h, with the temperature incrementally increasing at a rate of 2 °C per minute.

Figure 1. The mini form for obtaining zeolites in the form of granules.

Mechanical activation of the zeolite specimens was carried out using a high-energy planetary grinder (model XQM-0.4A, Tencan, Changsha, China) operating at 800 rpm for 60 min. Stainless steel balls of varying diameters (5–30 mm) served as the grinding media, with a media-to-zeolite mass ratio of 6:1. This activation process aimed to enhance the available surface area and create additional reactive sites for improved CO_2 capture.

The chemical modification of the zeolites was performed by incorporating 2 wt.% of magnesium oxide (MgO), sodium oxide (Na_2O), or lithium oxide (Li_2O) relative to the total mass of the zeolite, resulting in a final concentration of 98 wt.% zeolite in each modified sample. Chemical modification of the zeolites was carried out by the mechanical mixing of zeolite and salts (magnesium nitrate, lithium nitrate, and sodium carbonate). The resulting mixtures were mixed with deionized water to form a paste, which was placed in a mini mold. Samples using magnesium nitrate and sodium carbonate were calcined at 600 °C with a heating rate of 2 °C per min. The sample with lithium nitrate was dried at 200 °C for 2 h and then calcined at 750 °C for 3 h. Figure 2 shows photographic images of the samples before and after calcination.

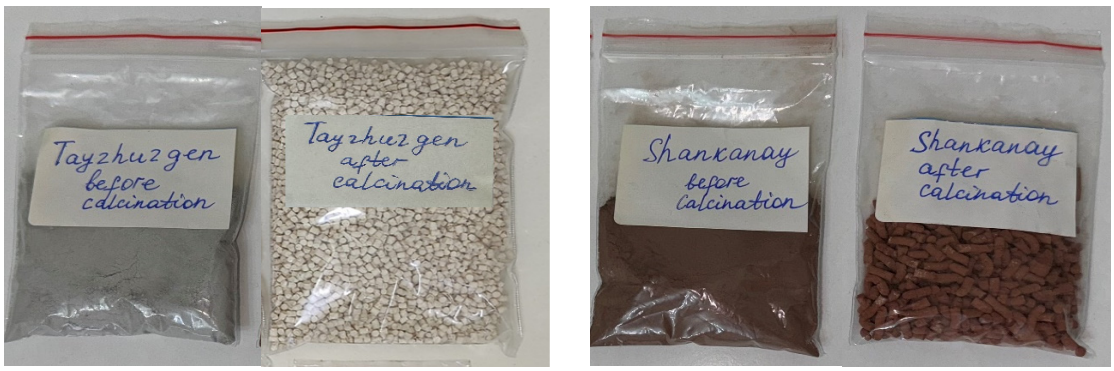

Figure 2. Photographic images of samples before and after calcination.

The study of the sorption properties of natural zeolites was conducted using a laboratory-scale flow system. The setup includes a reactor, thermocouple, electric furnace, control unit, and gas flow regulation system. For the experiments, CO_2 (supplied by LLP "Ihsan Technogas", with 99.99% purity) was used as the adsorbate, and He was used as a carrier gas to flush the line from the reactor to the chromatograph (also supplied by LLP "Ihsan Technogas", with 99.99% purity). The reactor was made of quartz glass with an inner diameter of 10 mm and a length of 25 cm. A 2 mL sample of sorbent was weighed and placed in a fixed bed within the reactor. CO_2 adsorption on natural zeolites (Tg) and

(Sh) was conducted at temperatures of 25 °C, 150 °C, 300 °C, and 500 °C over a period of 30 min, with CO_2 flowing at a rate of 15 mL/min. Subsequently, CO_2 desorption was performed at 700 °C for 30 min. The amount of CO_2 adsorbed by each sample during the experiments was measured using chromatographic analysis with a Chromos GC-1000 gas chromatograph equipped with a thermal conductivity detector (TCD).

To characterize the zeolite samples, their specific surface area was determined using low-temperature nitrogen adsorption at 77 K (BEL Japan Inc., Toyonaka, Japan) on a BELSORP-mini II analyzer. Prior to the measurements, the samples were degassed at elevated temperatures to remove adsorbed gasses and vapors.

The morphology of the samples was studied using a low-vacuum scanning electron microscope (JSM-6490 LA, Jeol Ltd., Tokyo, Japan) equipped with an energy-dispersive X-ray analysis (EDX) system. The primary electron beam was generated by a heated tungsten filament or a field emission gun and accelerated with a voltage ranging from 1 to 30 kV. Electromagnetic lenses were used to focus the beam on a nanometer-scale spot. The surface morphology of the samples was analyzed using data acquired from a secondary electron detector.

The phase composition analysis was performed using a DRON-3 automated diffractometer with CuKα radiation (β-filter). The measurement conditions included a tube voltage of 35 kV, a tube current of 20 mA, a θ–2θ scan mode, and a detector speed of 2 °/min. Semi-quantitative analysis was carried out on powder diffraction patterns using the equal-weight method and artificial mixtures. Data interpretation was conducted with the PDF-2 database (Release 2022) and HighScore Plus software (version 4.7).

The structural analysis of the samples was performed using Raman spectroscopy on a Solver Spectrum instrument (NT-MDT). A 473 nm laser was used as the excitation source and focused on the sample through a 100× objective, creating a spot size of 2 μm. The signal was recorded using a 600/600 diffraction grating, providing a spectral resolution of 4 cm^{-1}.

The basicity of the sorbent surface was evaluated using CO_2 temperature-programmed desorption (TPD) on a UNISIT chemisorption analyzer (USGA-101, Moscow, Russia). A 0.06 g powdered sample was placed in a quartz reactor, secured between quartz wool plugs, and preheated at 500 °C for 2 h under a helium flow. The surface of the sample was subsequently saturated with CO_2 (20 mL/min) at room temperature for 30 min. After removing weakly adsorbed CO_2 by purging with helium at 50 °C for 30 min, the desorption process was performed by heating the sample to 800 °C at a ramp rate of 10 °C/min in a helium flow of 20 mL/min.

The elemental composition of the studied samples was determined using energy-dispersive X-ray fluorescence spectrometry (EDXRF) on a NEX CG II spectrometer (Rigaku, Tokyo, Japan). The analysis was conducted in a helium atmosphere with the use of five secondary targets: Al, Mo, Cu, RX9, and Si. The operational parameters of the spectrometer were as follows: tube voltage—50 kV (for Al, Mo, and Cu) and 25 kV (for RX9 and Si); tube current—1 mA (for Al, Mo, and Cu) and 2 mA (for RX9 and Si); exposure time—100 s (for Al, Mo, and Cu) and 200 s (for RX9 and Si). Prior to the analysis, the samples were finely ground using an agate mortar to ensure homogeneity. The powder samples were prepared for analysis using 4-micron polypropylene film. This methodology ensured high accuracy and the reproducibility of the results. The designation of sorbents is provided in Table 1.

Table 1. Designation of sorbents.

Samples	Abbreviation
Zeolite Shankanay	Sh
Zeolite Tayzhuzgen	Tg
Zeolite Tayzhuzgen mechanically activated at 6:1	Tg 6:1

The CO_2 adsorption capacity in each experiment was determined using a model to quantify the amount of CO_2 adsorbed by the sorbent. The adsorption capacity, denoted as q (mmol CO_2/g), was calculated based on the following equation [21]:

$$q = \frac{Q \times P_{CO2}}{m \times M_w} \times \int_0^1 \left(\frac{C_0 - C}{1 - C}\right) dt \times \frac{T_0}{T} \quad (1)$$

In this equation: q is the adsorption capacity (mmol CO_2/g); Q represents the volumetric flow rate of the gas (mL/min); P_{CO2} is the density of CO_2 (g/cm^3); *m* is the mass of the adsorbent (g); M_W denotes the molecular weight of CO_2 (mg/mmol); C_0 and C correspond to the CO_2 concentrations at the reactor inlet and outlet (%), respectively; T_0 is the reference temperature (°C); T is the experimental temperature (°C); *t* represents the time of adsorption (min).

3. Results

Table 2 provides the composition analysis of zeolites obtained from the Tayzhuzgen (Tg) and Shankanay (Sh) sites. These data highlight the variation in the composition between the two deposits, particularly in terms of the relative concentrations of major oxides such as aluminum oxide (Al_2O_3), silicon dioxide (SiO_2), and calcium oxide (CaO). For the zeolite from the Tg deposit, a high SiO_2 content of 72.2 wt.% and an Al_2O_3 content of 12.9 wt.% were observed, alongside smaller quantities of calcium oxide (5.6 wt.%) and trace amounts of zinc oxide (ZnO) and indium oxide (In_2O_3). In contrast, the Sh deposit zeolite exhibited a significantly higher CaO content (15.2 wt.%) and notable levels of Fe_2O_3 (14.7 wt.%), while lacking the zinc and indium oxides found in the Tayzhuzgen zeolite [22].

Table 2. Elemental analysis of zeolites from Tg and Sh sites.

Composition, wt.%	Al_2O_3	SiO_2	CaO	ZnO	In_2O_3	Fe_2O_3	K_2O
Tg	12.9	72.2	5.6	1.2	7.7	0.4	-
Sh	16.9	49.5	15.2	-	-	14.7	3.7

A critical factor in evaluating zeolite structure is the silicon-to-aluminum (Si/Al) ratio. The results indicate that the zeolites from the Tayzhuzgen deposit have a significantly higher silicon-to-aluminum ratio of 5.6, in contrast to the Shankanay deposit, where the ratio is lower at 2.9.

The Si/Al ratio of 5.6 observed for the Tayzhuzgen (Tg) zeolite indicates a relatively high silica content, which is consistent with partially dealuminated natural clinoptilolites. Similar values have been reported in the literature for clinoptilolite samples from other deposits, such as Khonguruu, where Si/Al ratios of up to 5.57 have been recorded [23]. This elevated ratio may result from the unique geological conditions of the Tayzhuzgen deposit, leading to a higher degree of silica enrichment. Additionally, such a ratio aligns with the characteristics of clinoptilolites known to exhibit improved thermal stability and CO_2 adsorption efficiency due to enhanced framework basicity.

Following mechanical activation, the zeolite from the Tg deposit, characterized by a high Si/Al ratio, showed a significant improvement in its specific surface area. The BET analysis demonstrated an increase from 11.1 m^2/g to 16.0 m^2/g, as outlined in Table 3, indicating the enhanced textural properties of the material post activation.

Table 3. The textural characteristics of the zeolites.

Samples	Surface Area, m^2/g
Sh	5.61
Tg	11.12
Tg 6:1	16.0

Upon mechanical activation, the intensity of this band increases significantly, indicating a greater dispersion of the zeolite particles and enhanced structural changes. Further analysis of the particle morphology was conducted using scanning electron microscopy (SEM), providing detailed insights into the physical modifications induced by the mechanical treatment (Figure 3).

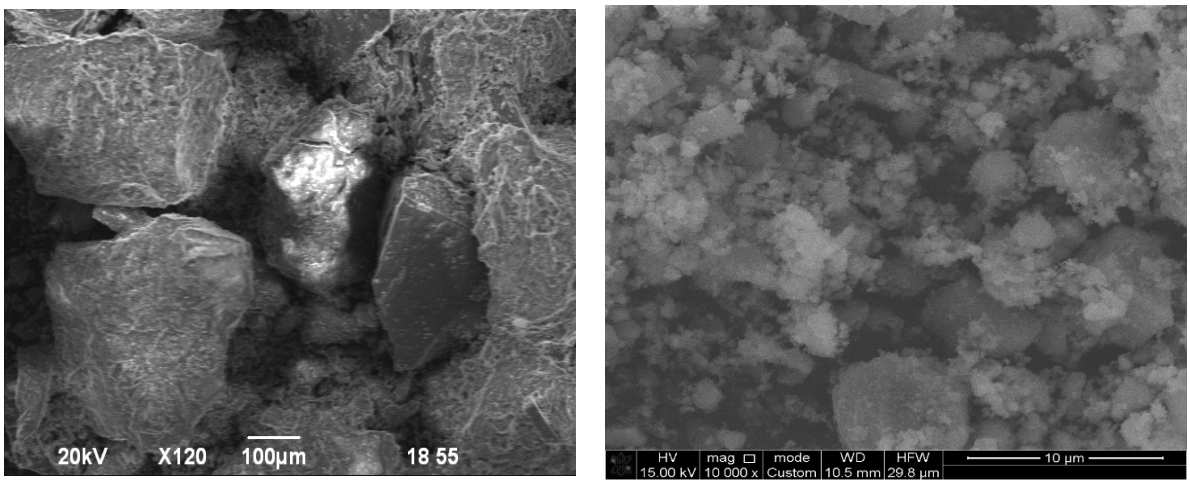

(**a**) (**b**)

Figure 3. SEM micrographs: (**a**) Tg; (**b**) Tg 6:1.

The SEM images reveal distinct morphological differences between the mechanically activated and non-activated samples of the zeolite from the Tayzhuzgen deposit (Tg). In the non-activated sample, zeolite particles appear as aggregates of various shapes and sizes, ranging from 100 to 500 µm. However, after mechanical activation, there is a notable reduction in particle size to a range of 0.2 to 6.45 µm, resulting in a more homogeneous and finely dispersed distribution. The images primarily depict amorphous particles within this size range. Figure 4 presents the phase characteristics of the zeolite, comparing its structure prior to and following mechanical activation, and emphasizing the structural changes brought about by this process.

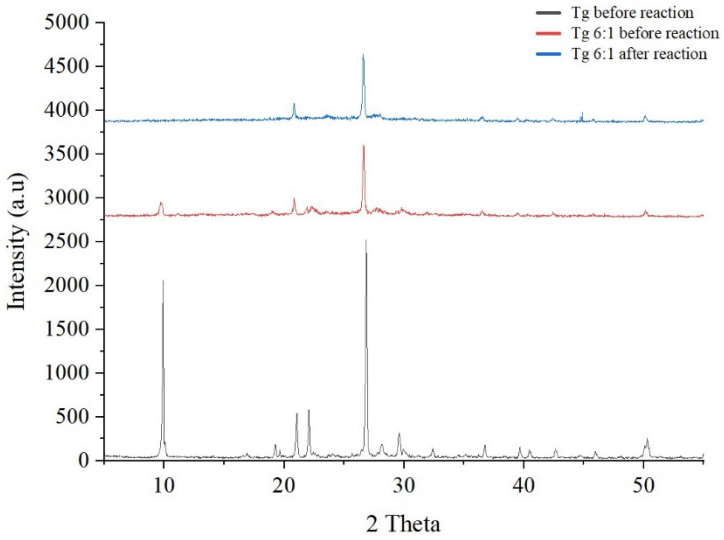

Figure 4. XRD profiles of Tg zeolite pre- and post-reaction.

The X-ray diffraction (XRD) pattern of the Tayzhuzgen (Tg) zeolite prior to mechanical activation displays distinct reflections at 9.9°, 19.03°, 22.3°, 26.8°, 28.3°, 29.5°, 32.4°, 36.6°,

39.7°, 40.4°, 42.7°, 45.8°, and 50.3°. These peaks are characteristic of the presence of clinoptilolite, consistent with reference data from JCPDS card 3-0427. As documented in prior studies [24–26], the most prominent peaks for crystalline clinoptilolite typically occur at diffraction angles 2θ: 9.86°, 11.06°, 13.03°, 14.82°, 16.86°, 17.2°, 19.04°, 22.35°, 25.04°, 28.09°, 31.71°, and 32.67°. Following mechanical activation, the intensity of these reflections diminishes, which can be attributed to the increased structural disorder and the emergence of amorphous phases caused by the milling process. These changes indicate a breakdown of the crystalline structure, leading to the amorphization of the material. Additional phase characterization was performed using Raman spectroscopy, as shown in Figure 5.

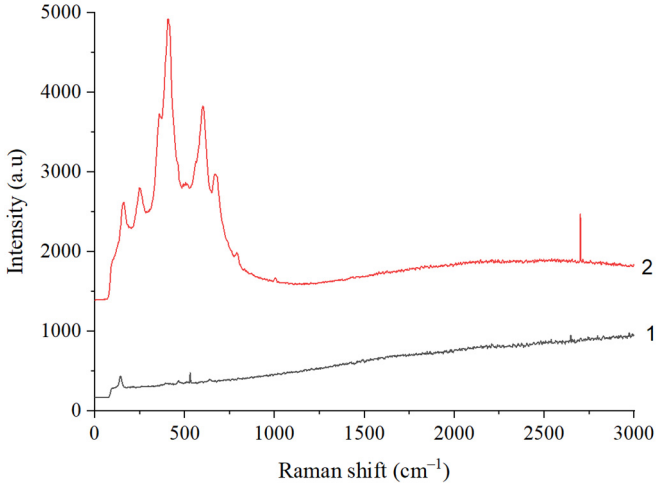

Figure 5. Raman spectra of samples: 1—Tg with mechanical activation before reaction; 2—Tg without mechanical activation, 6:1 before reaction.

The Raman spectrum shows characteristic peaks at 408, 488, and 604 cm^{-1}, suggesting clinoptilolite within the zeolite framework, consistent with findings reported in previous studies [27]. After mechanical activation, a notable reduction in the intensity of these peaks is observed, attributed to the formation of amorphous phases within the zeolite. It is well-established [28,29] that the increased dispersion of particles leads to higher defect densities, resulting in a less pronounced spectral response.

The sorption capacity of zeolites can be enhanced by incorporating various modifying additives into their structure. The most effective modifiers are compounds of alkali and alkaline earth metals [30,31]. Therefore, the mechanically activated Tg zeolite was modified using magnesium, lithium, and sodium compounds. The modified sorbents were evaluated in a flow reactor under atmospheric pressure, targeting CO_2 capture. Adsorption capacity was assessed over various temperatures, spanning 50 °C to 500 °C, including intermediate points at 150 °C and 300 °C. Figure 6 presents a comparative analysis of the sorption properties of Shankanay (Sh) zeolite, as well as non-activated and mechanically activated Tg zeolite, under the specified conditions.

When comparing the CO_2 sorption capacities of non-activated zeolites sourced from deposits at Tg and Sh, it is evident that the Tg zeolite exhibits superior sorption capabilities. Mechanical activation of the Tg zeolite results in a slight enhancement in CO_2 sorption capacity, attributed to the increased dispersion of the zeolite particles. The increase in the dispersion of Tg zeolite particles after mechanical activation is confirmed by the results of XRD and Raman spectroscopy. Modification with magnesium, lithium, and sodium oxides leads to a change in the sorption capacity of the Tg zeolite. The CO_2 sorption capacity of the sorbents is presented in Figure 7.

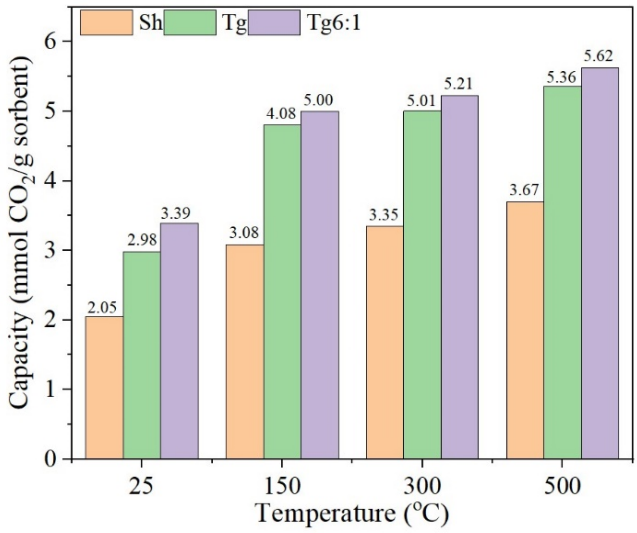

Figure 6. CO_2 sorption capacity of natural zeolite.

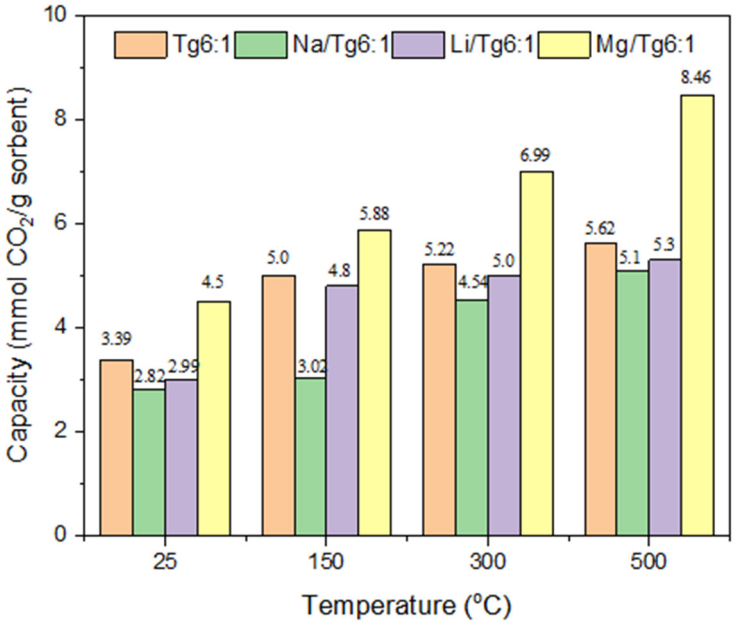

Figure 7. CO_2 sorption capacity of sorbents.

The incorporation of sodium and lithium carbonates into the Tg zeolite composition results in a reduction in sorption capacity across all adsorption temperatures. Introducing magnesium carbonate results in a notable enhancement of the sorption capacity of the Tg zeolite [32,33]. Comparison of the CO_2 adsorption capacity of magnesium-containing samples derived from natural zeolite from the Tg deposit with other magnesium-based sorbents (Table 4) indicates that the MgO/Tg 6:1 sorbent demonstrates excellent adsorption capacity at elevated temperatures relative to other magnesium-based materials.

Figure 8 illustrates the comparison of the phase composition of the sorbents before and after CO_2 adsorption and desorption.

Table 4. Comparison of CO_2 adsorption capacity on magnesium-containing adsorbents.

Composition of Sorbents	Preparation Methods	CO_2 Adsorption Temperature/°C	Adsorption Time (min)	Adsorption Capacity (wt. %)/mmol/g	Ref./This Work
Mg-MOF-74	sonochemical method	25	-	35%	[34]
MgO/K_2CO_3	recipitation method	375	120	8.7	[35]
MgO-BM2.5h	solution–combustion	25 and 1 atm	30	1.611 mmol/g	[36]
MgO	sol–gel	30	-	0.68	[37]
PEI-MgO	sol–gel and impregnation	30	-	0.54 mmol/g	
$MgO-SiO_2$	acid leaching	75	-	0.41 mmol/g	[38]
$MgO{\cdot}KNO_3$	aerogel method	325	120	13.9%	[39]
MgO/Tg 6/1	capillary impregnation	500	30	8.46 mmol/g	[This work]
$MgO-CeO_2$	sol–gel combustion	325	240	45%	[40]
Calcinated magnesite MgO	-	60 °C, 0.4 МПа	-	1.82 mmol/g	[41]
$MgO{\cdot}Na_2CO_3$	aerogel method	325	240	4.3%	[42]
MgO	aerogel method	30	5	10%	[43]
MgO-SR	solid-state chemical reaction method	60	-	2.39 mmol/g	[22]
Mg-ZK-5	ion exchanges	30, 0.15 bar	-	1.9 mmol/g	[44]
Mg-CHA	ion exchanges	−0.15–60 0.15 bar	-	3.4 mmol/g	[31]

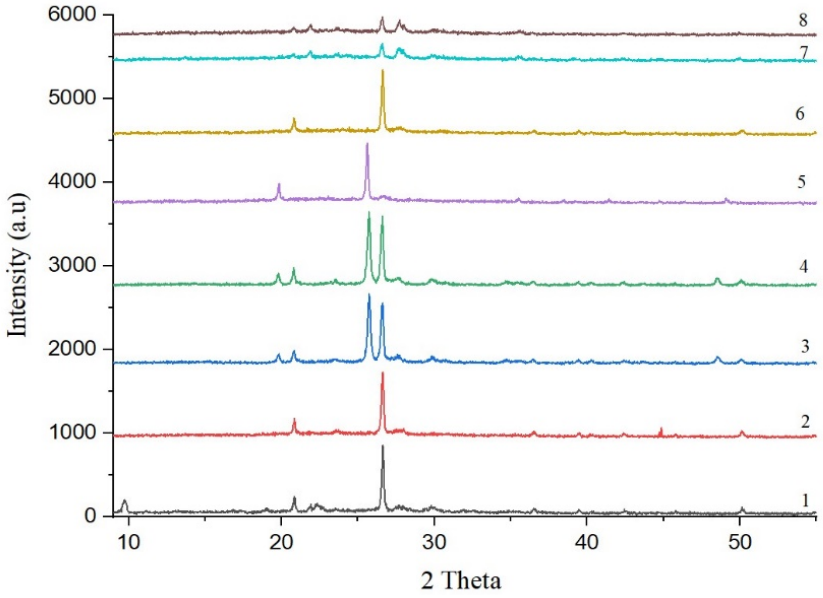

Figure 8. X-ray diffraction of samples: 1—Tg 6:1 before; 2—Tg 6:1 after; 3—Li_2O/Tg 6:1 before; 4—Li_2O/Tg 6:1 after; 5—MgO/Tg 6:1 before; 6—MgO/Tg 6:1 after; 7—Na_2O/Tg 6:1 before; 8—Na_2O/Tg 6:1 after.

Reflections at 20°, 26.6°, and 50°, observed in all sorbents, correspond to the SiO_2 phase [45–47]. The addition of lithium oxide leads to the appearance of an intense peak at 27.5°, which is attributed to the formation of $Li_xAl_xSi_{1-x}O_2$ [48–50]. The addition of sodium carbonate leads to a reduction in the SiO_2 peak intensity, possibly as a result of the enhanced amorphous characteristics of the sorbent particles. Peaks observed at 21.8°, 23.6°, 27.6°, 29.8°, 35.5°, 39.1°, and 49.8° correspond to the $NaAlSi_3O_8$ phase. According to the literature, lithium aluminosilicates are less effective as sorbents for CO_2 capture compared to lithium orthosilicate. This is due to the more complex structure and lower surface activity of lithium aluminosilicates, which can lead to a decrease in sorption capacity [51–54]. The addition of magnesium oxide to zeolite results in the formation of the

$CaMg(Si_2O_6)$ phase. $CaMg(Si_2O_6)$ is a typical binary compound formed from calcium and magnesium silicates, and it can be synthesized via the following reaction: $CaO + MgCO_3 + 2SiO_2 = CaMg(Si_2O_6) + CO_2$ [55]. $CaMg(Si_2O_6)$ demonstrates a high capacity for CO_2 adsorption. As shown in [56], during the grinding of $CaMg(Si_2O_6)$, deep carbonation occurs due to the adsorption of CO_2 from the surrounding atmosphere, with the adsorbed CO_2 present in the form of carbonate ions. These ions are likely associated with calcium and magnesium cations within the silicate material. The reaction between carbon dioxide and $CaMg(Si_2O_6)$ proceeds according to the following equation [55,57]:

$$CaMg(Si_2O_6) + 2CO_2 = CaCO_3 + MgCO_3 + 2SiO_2 \quad (2)$$

However, in the XRD spectra of the MgO/Tg 6:1 sample after CO_2 desorption, no reflections corresponding to $CaCO_3$ or $MgCO_3$ were observed. Instead, reflections from the SiO_2, MgO, and $MgSiO_3$ phases were detected. These data suggest that at a desorption temperature of 700 °C, magnesium carbonate may decompose further into magnesium oxide and carbon dioxide [58,59]. The decomposition temperature of calcium carbonate is significantly higher, around 900 °C or more, so in our experimental conditions, it is unlikely to decompose further [60,61]. The absence of $CaCO_3$ reflections in the spent samples may be attributed to its low content. The formation of $MgSiO_3$ is likely due to several reactions, including the following [62,63]:

$$MgCO_3 + SiO_2 = MgSiO_3 + CO_2 \quad (3)$$

$$MgO + SiO_2 = MgSiO_3 \quad (4)$$

Identification of the MgO/Tg 6:1, Na_2O/Tg 6:1, and Li_2O/Tg 6:1 phases was carried out by Raman spectroscopy (Figure 9).

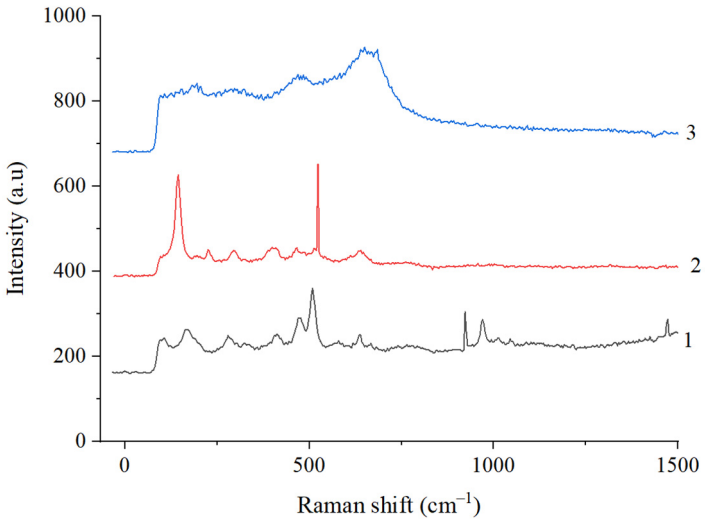

Figure 9. Raman spectra of samples before reaction: 1—Na_2O/Tg 6:1; 2—Li_2O/Tg 6:1; 3—MgO/Tg 6:1.

In the spectrum of Li_2O/Tg 6:1 prior to reaction, distinct bands are observed at 140, 232, 290, 398, 526, and 639 cm^{-1}. The peak in the range of 232–526 cm^{-1} is associated with vibrations of oxygen ions and the bonds between lithium and oxygen ions in the Li-O bond. The band observed at 600 cm^{-1} is associated with the vibrations of Al–O–Al bonds and may correspond to $Li_xAl_xSi_{1-x}O_2$ [50,64].

In this instance of MgO/Tg 6:1, the corresponding bands can be as follows: 99–107, 466, 653–684 cm^{-1}. The peak at 653 cm^{-1} is due to Si-O-Si intertetrahedral bonds and can be detected in both calcium and magnesium silicates [65–67]. The spectrum of Na_2O/Tg 6:1 is characterized by bands at 473, 505, 639, 922, and 966 cm^{-1}. The bands within 200 to 639 cm^{-1} are indicative of intertetrahedral T–O–T (T = Si or Al) vibrational modes. Mean-

while, the band between 922 and 966 cm^{-1} corresponds to the T–O stretching vibrations in $NaAlSi_3O_8$ [68].

The main properties of the investigated sorbents were studied using the TPD-CO_2 method (Figure 10). According to the literature, weak basic sites are observed in the low-temperature range (50–175 °C), medium basic sites in the range of 175–400 °C, while strong basic sites are characterized by desorption at high temperatures exceeding 400 °C [69].

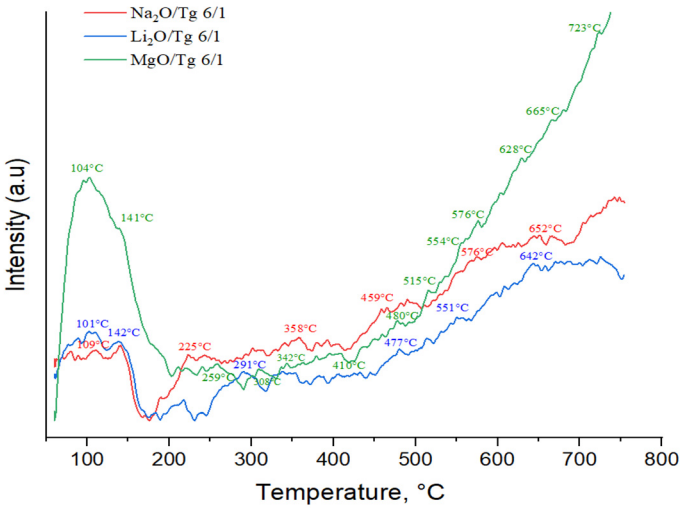

Figure 10. TPD-CO_2 sorbent profiles.

The TPD-CO_2 results indicate that the intensity of the peaks associated with weak basic sites (50–175 °C) on the Na_2O/Tg 6:1 sorbent is lower than that on Li_2O/Tg 6:1 and MgO/Tg 6:1. However, in the medium-temperature range (175–400 °C), the desorption peak intensity on Na_2O/Tg 6:1 exceeds that of Li_2O/Tg 6:1 and MgO/Tg 6/1, indicating a more pronounced presence of medium basic sites. The MgO/Tg 6:1 sorbent exhibits the highest intensity of CO_2 desorption peaks in both the 50–175 °C and above 400 °C temperature ranges.

The presence of weak basic sites is associated with surface hydroxyl groups [70]. The medium basic sites are related to metal ions (Mg^{2+}, Na^+, Li^+) and O^{2-}, where CO_2 adsorption occurs. Strong basic sites correspond to low-coordinate oxide sites that interact with CO_2, resulting in the formation of bidentate and/or monodentate carbonates [71]. The TPD-CO_2 results showed that MgO/Tg 6:1 exhibits the highest overall basicity compared to Na_2O/Tg 6:1 and Li_2O/Tg 6:1, which positively influences its sorption capacity.

CO_2 adsorption on zeolites involves both physical and chemical processes, the efficiency of which depends on the zeolite structure and its chemical modification [72]. Physical adsorption is mainly governed by the interaction of CO_2 molecules with the surface of the material through van der Waals forces [73], where CO_2 molecules are retained on the zeolite surface via weak non-covalent interactions. In contrast, chemical adsorption involves the interaction of CO_2 molecules with active sites on the zeolite surface, leading to the formation of strong chemical bonds, including carbonate compounds. This process ensures more reliable retention of CO_2 molecules and contributes to effective gas capture, especially at elevated temperatures. Furthermore, the modification of zeolites with various metal oxides can significantly enhance their adsorption properties by creating additional active sites on the surface. The mechanism of CO_2 adsorption on the MgO/Tayzhuzgen 6:1 sorbent is illustrated in Figure 11. The dashed lines represent coordination bonds formed between Mg^{2+} and the oxygen atoms on the surface of the sorbent.

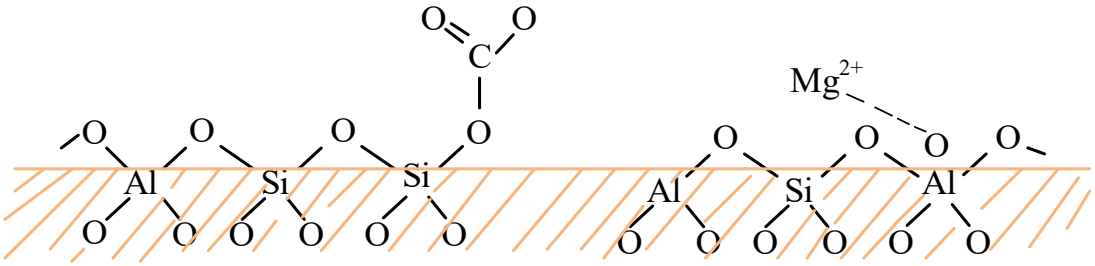

Figure 11. Mechanism of CO_2 adsorption on the MgO/Tayzhuzgen 6:1 sorbent.

The addition of magnesium oxide (MgO) to the zeolite surface creates active sites in the form of Mg^{2+} and O^{2-} ions, which significantly enhance the sorption capacity of the sorbent. The adsorption process begins with the physical interaction of CO_2 molecules with the zeolite surface. However, the key role in CO_2 retention is played by chemical adsorption, which occurs as a result of the reaction between CO_2 molecules and the active sites of MgO. The CO_2 molecules interact with Mg^{2+} and O^{2-} ions on the surface, forming stable carbonate compounds, such as magnesium carbonate ($MgCO_3$). This chemical interaction ensures the strong retention of CO_2 on the sorbent surface, facilitating efficient gas capture at high temperatures. Thus, the efficiency of CO_2 adsorption on modified zeolites depends on the type of oxide used for modification.

4. Conclusions

This study evaluated the physicochemical properties and CO_2 adsorption capacities of natural zeolites from the Tayzhuzgen (Tg) and Shankanay (Sh) deposits. The Tayzhuzgen zeolite exhibited a Si/Al ratio of 5.6, indicating partial dealumination, which contributed to its enhanced structural stability and sorption efficiency. Mechanical activation improved the surface area and pore volume of the zeolite, further boosting its adsorption potential. The modification of the Tayzhuzgen zeolite with magnesium oxide (MgO/Tg) significantly enhanced its CO_2 adsorption capacity, reaching 8.46 mmol CO_2/g, owing to the formation of the $CaMg(Si_2O_6)$ phase and increased basic active sites. Among the tested modifications, MgO/Tg demonstrated the highest basicity and sorption capacity, making it a promising candidate for high-temperature CO_2 capture applications. These findings highlight the importance of understanding the textural and chemical properties of natural zeolites, particularly the role of the Si/Al ratio and surface modifications, in optimizing their adsorption performance. Future research should focus on scaling up the preparation of modified zeolites, testing their performance under industrially relevant conditions, and exploring their regeneration efficiency to ensure their viability in sustainable carbon capture technologies.

Author Contributions: Conceptualization, M.M.; methodology, M.M.; software, M.M.; validation, M.M., G.Y. and K.D.; formal analysis, M.M.; investigation, M.M.; resources, K.D.; data curation, M.M.; writing—original draft preparation, M.M. and G.Y.; writing—review and editing, M.M. and G.Y.; visualization, K.D.; supervision, G.Y.; project administration, M.M.; funding acquisition, M.M. All authors have read and agreed to the published version of the manuscript.

Funding: This research was funded by the Science Committee of the Ministry of Education and Science of the Republic of Kazakhstan (Grant No. AP15473268).

Data Availability Statement: Data are contained within the article.

Conflicts of Interest: The authors declare no conflict of interest.

References

1. Tong, D.; Zhang, Q.; Zheng, Y.; Caldeira, K.; Shearer, C.; Hong, C.; Qin, Y.; Davis, S.J. Committed emissions from existing energy infrastructure jeopardize 1.5 °C climate target. *Nature* **2019**, *572*, 373–377. [CrossRef] [PubMed]
2. Mortazavi, N.; Bahadori, M.; Marandi, A.; Tangestaninejad, S.; Moghadam, M.; Mirkhani, V.; Mohammadpoor-Baltork, I. Enhancement of CO_2 adsorption on natural zeolite, modified clinoptilolite with cations, amines and ionic liquids. *Sustain. Chem. Pharm.* **2021**, *22*, 100495. [CrossRef]
3. Gür, T.M. Carbon Dioxide Emissions, Capture, Storage and Utilization: Review of Materials, Processes and Technologies. *Prog. Energy Combust. Sci.* **2022**, *89*, 100965. [CrossRef]
4. Elena, T.C.; Skinner, J.; David, G.T. CO_2 Capture in Ionic Liquids: A Review of Solubilities and Experimental Methods. *J. Chem.* **2013**, *2013*, 1–16. [CrossRef]
5. Soo, X.Y.D.; Lee, J.J.C.; Wu, W.; Tao, L.; Wang, C.; Zhu, Q.; Bu, J. Advancements in CO_2 capture by absorption and adsorp-tion: A comprehensive review. *J. CO_2 Util.* **2024**, *81*, 102727. [CrossRef]
6. Gunawardene, O.H.P.; Gunathilake, C.A.; Kumar, V.; Amaraweera, S.M. Carbon Dioxide Capture through Physical and Chemical Adsorption Using Porous Carbon Materials: A Review. *J. Atmos.* **2022**, *13*, 397. [CrossRef]
7. Ayeleru, O.O.; Modekwe, H.U.; Onisuru, O.R.; Ohoro, C.R.; Akinnawo, C.A.; Olubambi, P.A. Adsorbent technologies and applications for carbon capture, and direct air capture in environmental perspective and sustainable climate action. *Sustain. Chem. Clim. Action.* **2023**, *3*, 100029. [CrossRef]
8. Davarpanah, E.; Armandi, M.; Hernández, S.; Fino, D.; Arletti, R.; Bensaid, S.; Piumetti, M. CO_2 capture on natural zeolite clinoptilolite: Effect of temperature and role of the adsorption sites. *J. Environ. Manag.* **2020**, *275*, 111229. [CrossRef]
9. Wang, Q.; Luo, J.; Zhong, Z.; Borgna, A. CO_2 capture by solid adsorbents and their applications: Current status and new trends. *Energy Environ. Sci.* **2011**, *4*, 42–55. [CrossRef]
10. Biblioteca, I.; Sambucci, M.; Valente, M. Zeolite-Clinoptilolite conditioning for improved heavy metals ions removal: A preliminary assessment. *Ceram. Int.* **2023**, *49*, 39649–39656. [CrossRef]
11. Sharma, P.; Sutar, P.P.; Xiao, H.; Zhang, Q. The untapped potential of zeolites in techno-augmentation of the biomaterials and food industrial processing operations: A review. *J. Future Foods* **2023**, *3*, 127–141. [CrossRef]
12. El Bojaddayni, I.; Emin Küçük, M.; El Ouardi, Y.; Jilal, I.; El Barkany, S.; Moradi, K.; Repo, E.; Laatikainen, K.; Ouammou, A. A review on synthesis of zeolites from natural clay resources and waste ash: Recent approaches and progress. *Miner. Eng.* **2023**, *198*, 108086. [CrossRef]
13. El-Arish, N.A.S.; Zaki, R.S.R.M.; Miskan, S.N.; Setiabudi, H.D.; Jaafar, N.F. Adsorption of Pb (II) from aqueous solution using alkaline-treated natural zeolite: Process optimization analysis. *Total Environ. Res. Themes* **2022**, *3–4*, 100015. [CrossRef]
14. Morante-Carballo, F.; Montalván-Burbano, N.; Carrión-Mero, P.; Espinoza-Santos, N. Cation Exchange of Natural Zeolites: Worldwide Research. *Sustainability* **2021**, *13*, 7751. [CrossRef]
15. Abdulina, S.A.; Sadenova, M.A.; Sapargaliev, E.M.; Utegenova, M.E. Peculiarities of zeolite mineral composition of Taizhuzgen deposit. *Vestnik KazNTU.* **2014**, *103*, 24–31. (In Russian)
16. Mambetova, M.; Dossumov, K.; Baikhamurova, M.; Yergaziyeva, G. Sorbents Based on Natural Zeolites for Carbon Dioxide Capture and Removal of Heavy Metals from Wastewater: Current Progress and Future Opportunities. *Processes* **2024**, *12*, 2071. [CrossRef]
17. Rakhym, A.B.; Seilkhanova, G.A.; Kurmanbayeva, T.S. Adsorption of Lead (II) Ions from Water Solutions with Natural Zeolite and Chamotte Clay. *Mater. Today Proc.* **2020**, *31*, 482–485. [CrossRef]
18. Vasilyanova, L.S.; Lazareva, E.A. Zeolites in Ecology. News of Science of Kazakhstan. 2016, pp. 61–85. Available online: https://nv.nauka.kz/wp-content/uploads/2016/04/nnk-2016-1.pdf (accessed on 13 September 2024). (In Russian).
19. Telkhozhayeva, M.; Seilkhanova, G.; Rakhym, A.; Imangaliyeva, A.B.; Akbayeva, D.N. Sorption of lead and cadmium ions from aqueous solutions using modified zeolite. *Chem. Bull. Kazakh. Natl. Univ.* **2018**, *91*, 16–22. [CrossRef]
20. Kuldeyev, E.; Seitzhanova, M.; Tanirbergenova, S.; Tazhu, K.; Doszhanov, E.; Mansurov, Z.; Azat, S.; Nurlybaev, R.; Berndtsson, R. Modifying Natural Zeolites to Improve Heavy Metal Adsorption. *Water.* **2023**, *15*, 2215. [CrossRef]
21. Guo, Y.; Tan, C.; Wang, P.; Sun, J.; Li, W.; Zhao, C.; Lu, P. Structure-performance relationships of magnesium-based CO_2 adsorbents prepared with different methods. *Chem. Eng. J.* **2020**, *379*, 122277. [CrossRef]
22. Mambetova, M.; Yergaziyeva, G.; Zhoketayeva, A. Physicochemical characteristics and carbon dioxide sorption properties of natural zeolites. *Combust. Plasma Chem.* **2023**, *21*, 81–87. [CrossRef]
23. Nikashina, V.A.; Streletskii, A.N.; Kolbanev, I.V.; Meshkova, I.N.; Grinev, V.G.; Serova, I.B.; Yusupov, T.S.; Shumskaya, L.G. Effect of mechanical activation on the properties of natural zeolites. *Inorg. Mater.* **2011**, *47*, 1341–1346. [CrossRef]
24. Beycioglu, A.; Aruntaş, H.Y.; Gencel, O.; Hagg Lobland, H.E.; Şamandar, A.; Brostow, W. Effect of Elevated Temperatures on Properties of Blended Cements with Clinoptilolite. *Mater. Sci.* **2016**, *22*, 548–552. [CrossRef]
25. Güngör, D.; Özen, S. Development and Characterization of Clinoptilolite-, Mordenite-, and Analcime-Based Geopolymers: A Comparative Study. *Case Stud. Constr. Mater.* **2021**, *15*, e00576. [CrossRef]
26. Hernandez, M.A.; Hernandez, G.I.; Portillo, R.; Rubio, E.; Petranovskii, V.; Alvarez, K.M.; Velasco, M.D.L.A.; Santamaría, J.D.; Tornero, M.; Paniagua, L.A. CO_2 Adsorption on Natural Zeolites from Puebla, México, by Inverse Gas Chromatography. *Separations* **2023**, *10*, 238. [CrossRef]

27. Tsai, Y.L.; Huang, E.; Li, Y.H.; Hung, H.T.; Jiang, J.H.; Liu, T.C.; Fang, J.N.; Chen, H.F. Raman Spectroscopic Characteristics of Zeolite Group Minerals. *Minerals* **2021**, *11*, 167. [CrossRef]
28. Dabizha, O.N.; Derbenova, T.V.; Khamova, T.V.; Shilova, O.A. Controlling the Sorption Activity of Clinoptilolites with Mechanical Activation. *Inorg. Mater.* **2021**, *57*, 399–408. [CrossRef]
29. Wu, F.; Li, H.; Yang, K. Effects of Mechanical Activation on Physical and Chemical Characteristics of Coal-Gasification Slag. *Coatings* **2021**, *11*, 902. [CrossRef]
30. Zheng, S.; Heydenrych, H.R.; Jentys, A.; Lercher, J.A. Influence of Surface Modification on the Acid Site Distribution of HZSM-5. *J. Phys. Chem. B.* **2002**, *106*, 9552–9558. [CrossRef]
31. Zhang, J.; Singh, R.; Webley, P.A. Alkali and Alkaline-Earth Cation Exchanged Chabazite Zeolites for Adsorption Based CO_2 Capture. *Microporous Mesoporous Mater.* **2008**, *111*, 478–487. [CrossRef]
32. Pang, H.; Sun, A.; Xu, H.; Xiao, G. Regenerable MgO-Based Sorbents for CO_2 Capture at Elevated Temperature and Pressure: Experimental and DFT Study. *Chem. Eng. J.* **2021**, *425*, 130675. [CrossRef]
33. Donat, F.; Müller, C.R. Prospects of MgO-Based Sorbents for CO_2 Capture Applications at High Temperatures. *Curr. Opin. Green Sustain. Chem.* **2022**, *36*, 100645. [CrossRef]
34. Yang, D.A.; Cho, H.Y.; Kim, J.; Yang, S.T.; Ahn, W.S. CO_2 Capture and Conversion Using Mg-MOF-74 Prepared by a Sonochemical Method. *Energy Environ. Sci.* **2012**, *5*, 6465–6473. [CrossRef]
35. Xiao, G.; Singh, R.; Chaffee, A.; Webley, P. Advanced Adsorbents Based on MgO and K_2CO_3 for Capture of CO_2 at Elevated Temperatures. *Int. J. Greenh. Gas Control* **2011**, *5*, 634–639. [CrossRef]
36. Elvira, G.B.; Francisco, G.C.; Víctor, S.M.; Alberto, M.L.R. MgO-Based Adsorbents for CO_2 Adsorption: Influence of Structural and Textural Properties on the CO_2 Adsorption Performance. *J. Environ. Sci.* **2017**, *57*, 418–428. [CrossRef]
37. Alkadhem, A.M.; Elgzoly, M.A.A.; Onaizi, S.A. Novel Amine-Functionalized Magnesium Oxide Adsorbents for CO_2 Capture at Ambient Conditions. *J. Environ. Chem. Eng.* **2020**, *8*, 103968. [CrossRef]
38. Ouyang, J.; Gu, W.; Zheng, C.; Yang, H.; Zhang, X.; Jin, Y.; Chen, J.; Jiang, J. Polyethyleneimine (PEI) Loaded MgO-SiO 2 Nanofibers from Sepiolite Minerals for Reusable CO_2 Capture/Release Applications. *Appl. Clay Sci.* **2018**, *152*, 267–275. [CrossRef]
39. Vu, A.-T.; Park, Y.; Jeon, P.R.; Lee, C.-H. Mesoporous MgO Sorbent Promoted with KNO3 for CO_2 Capture at Intermediate Temperatures. *Chem. Eng. J.* **2014**, *258*, 254–264. [CrossRef]
40. Jin, S.; Ko, K.-J.; Lee, C.-H. Direct Formation of Hierarchically Porous MgO-Based Sorbent Bead for Enhanced CO_2 Capture at Intermediate Temperatures. *Chem. Eng. J.* **2019**, *371*, 64–77. [CrossRef]
41. Yang, N.; Ning, P.; Li, K.; Wang, J. MgO-Based Adsorbent Achieved from Magnesite for CO 2 Capture in Simulate Wet Flue Gas. *J. Taiwan Inst. Chem. Eng.* **2018**, *86*, 73–80. [CrossRef]
42. Vu, A.T.; Ho, K.; Jin, S.; Lee, C.H. Double Sodium Salt-Promoted Mesoporous MgO Sorbent with High CO_2 Sorption Capacity at Intermediate Temperatures under Dry and Wet Conditions. *Chem. Eng. J.* **2016**, *291*, 161–173. [CrossRef]
43. Ho, K.; Jin, S.; Zhong, M.; Vu, A.T.; Lee, C.H. Sorption Capacity and Stability of Mesoporous Magnesium Oxide in Post-Combustion CO_2 Capture. *Mater. Chem. Phys.* **2017**, *198*, 154–161. [CrossRef]
44. Liu, Q.; Pham, T.; Porosoff, M.D.; Lobo, R.F. ZK-5: A CO_2 Selective Zeolite with High Working Capacity at Ambient Temperature and Pressure. *Chem. Sus. Chem.* **2012**, *5*, 2237–2242. [CrossRef]
45. Olegario-Sanchez, E.; Felizco, J.C.; Mulimbayan, F. Investigation of the Thermal Behavior of Philippine Natural Zeolites. In Proceedings of the AIP Conference, Langkawi, Malaysia, 4 December 2017; p. 070005.
46. Joni, I.M.; Nulhakim, L.; Vanitha, M.; Panatarani, C. Characteristics of Crystalline Silica (SiO2) Particles Prepared by Simple Solution Method Using Sodium Silicate (Na2SiO3) Precursor. *J. Phys. Conf. Ser.* **2018**, *1080*, 012006. [CrossRef]
47. Rahmadhani, D.; Yuliani, K.D.; Frida, E.; Taufiq, A. Hydrophobic and Antibacterial Properties of Textiles Using Nanocomposite Chitosan and SiO2 from Rice Husk Ash As-Coating. *S. Afr. J. Chem. Eng.* **2024**, *48*, 366–374. [CrossRef]
48. Guo, X.; Yang, H.; Han, C.; Song, F. Crystallization and Microstructure of Li2O–Al2O3–SiO2 Glass Containing Complex Nucleating Agent. *Thermochim. Acta* **2006**, *444*, 201–205. [CrossRef]
49. Kleebusch, E.; Patzig, C.; Krause, M.; Hu, Y.; Höche, T.; Rüssel, C. The Formation of Nanocrystalline ZrO2 Nuclei in a Li2O-Al2O3-SiO2 Glass—A Combined XANES and TEM. *Study Sci. Rep.* **2017**, *7*, 10869. [CrossRef]
50. Naumov, A.S.; Shakhgildyan, G.Y.; Golubev, N.V.; Lipatiev, A.S.; Fedotov, S.S.; Alekseev, R.O.; Ingat'eva, E.S.; Savinkov, V.I.; Sigaev, V.N. Tuning the Coefficient of Thermal Expansion of Transparent Lithium Aluminosilicate Glass-Ceramics by a Two-Stage Heat Treatment. *Ceramics* **2023**, *7*, 1–14. [CrossRef]
51. Wang, K.; Guo, X.; Zhao, P.; Wang, F.; Zheng, C. High Temperature Capture of CO_2 on Lithium-Based Sorbents from Rice Husk Ash. *J. Hazard. Mater.* **2011**, *189*, 301–307. [CrossRef]
52. Sanna, A.; Thompson, S.; Zajac, J.M.; Whitty, K.J. Evaluation of Palm-Oil Fly Ash Derived Lithium Silicate for CO_2 Sorption under Simulated Gasification Conditions. *J. CO_2 Util.* **2022**, *56*, 101826. [CrossRef]
53. Hernández-Palomares, A.; Alcántar-Vázquez, B.; Ramírez-Zamora, R.M.; Coutino-Gonzalez, E.; Espejel-Ayala, F. CO_2 Capture Using Lithium-Based Sorbents Prepared with Construction and Demolition Wastes as Raw Materials. *Mater. Today Sustain.* **2023**, *24*, 100491. [CrossRef]
54. Li, P.; Jiang, Z.; Guo, H.; Zhao, W.; Zheng, F.; Chen, Y.; Yan, B.; Chen, D. Lithium Based High Temperature Sorbent from Copper Slag: Synthesis and CO_2 Capture Performance. *Ceram. Int.* **2023**, *49*, 37435–37444. [CrossRef]

55. Chai, Y.E.; Chalouati, S.; Fantucci, H.; Santos, R.M. Accelerated Weathering and Carbonation (Mild to Intensified) of Natural Canadian Silicates (Kimberlite and Wollastonite) for CO_2 Sequestration. *Crystals* **2021**, *11*, 1584. [CrossRef]
56. Kalinkin, A.M.; Kalinkina, E.V.; Zalkind, O.A.; Makarov, V.N. CO_2 Sorption during Mechanical Activation of Sodium and Calcium Aluminosilicates. *Inorg. Mater.* **2005**, *41*, 486–491. [CrossRef]
57. Paustian, K.; Pacala, S.W.; Al-Kaisi, M.; Barteau, M.A.; Belmont, E.; Benson, S.M.; Birdsey, R.; Boysen, D.; Duren, R.M.; Hopkinson, C.; et al. *Negative Emissions Technologies and Reliable Sequestration: A Research Agenda*; National Academies Press: Washington, DC, USA, 2019; p. 25259. ISBN 978-0-309-48452-7.
58. Hu, Y.; Liu, X.; Zhou, Z.; Liu, W.; Xu, M. Pelletization of MgO-Based Sorbents for Intermediate Temperature CO_2 Capture. *Fuel* **2017**, *187*, 328–337. [CrossRef]
59. Papalas, T.; Polychronidis, I.; Antzaras, A.N.; Lemonidou, A.A. Enhancing the Intermediate-Temperature CO_2 Capture Efficiency of Mineral MgO via Molten Alkali Nitrates and CaCO3: Characterization and Sorption Mechanism. *J. CO_2 Util.* **2021**, *50*, 101605. [CrossRef]
60. López-Periago, A.M.; Fraile, J.; López-Aranguren, P.; Vega, L.F.; Domingo, C. CO_2 Capture Efficiency and Carbonation/Calcination Kinetics of Micro and Nanosized Particles of Supercritically Precipitated Calcium Carbonate. *Chem. Eng. J.* **2013**, *226*, 357–366. [CrossRef]
61. Jiang, P.; Zhang, H.; Zhao, G.; Li, L.; Ji, T.; Mu, L.; Lu, X.; Zhu, J. A Thermodynamic View on the In-Situ Carbon Dioxide Reduction by Biomass-Derived Hydrogen during Calcium Carbonate Decomposition. *Chin. J. Chem. Eng.* **2024**, *68*, 231–240. [CrossRef]
62. Litasov, K.D.; Shatskiy, A.F. MgCO3 + SiO2 Reaction at Pressures to 32 GPa Studied Using in Situ X-Ray Diffraction and Synchrotron Radiation. *Geochemistry* **2019**, *64*, 1003–1012. [CrossRef]
63. Kwon, S.H.; Hiremath, V.; Nanoti, A.; Kang, S.G.; Seo, J.G.; Lee, S.G. MgO-Based Composites for High Pressure CO_2 Capture: A First-Principles Theoretical and Experimental Investigation. *Korean J. Chem. Eng.* **2023**, *40*, 2990–2996. [CrossRef]
64. Blanco-García, S.; Aguado, F.; González, J.; Rodriguez, F. A Raman Study of the Pressure-Induced Densification of SiO2 -Based Glass-Ceramics. *J. Phys. Condens. Matter.* **2018**, *30*, 304002. [CrossRef] [PubMed]
65. Cormier, L.; Cuello, G.J. Structural Investigation of Glasses along the MgSiO3–CaSiO3 Join: Diffraction Studies. *Geochim. Cosmochim. Acta* **2013**, *122*, 498–510. [CrossRef]
66. Moulton, B.J.A.; Henderson, G.S.; Fukui, H.; Hiraoka, N.; De Ligny, D.; Sonneville, C.; Kanzaki, M. In Situ Structural Changes of Amorphous Diopside (CaMgSi2O6) up to 20 GPa: A Raman and O K-Edge X-Ray Raman Spectroscopic Study. *Geochim. Cosmochim. Acta* **2016**, *178*, 41–61. [CrossRef]
67. Morizet, Y.; Trcera, N.; Larre, C.; Rivoal, M.; Le Menn, E.; Vantelon, D.; Gaillard, F. X-Ray Absorption Spectroscopic Investigation of the Ca and Mg Environments in CO_2-Bearing Silicate Glasses. *Chem. Geol.* **2019**, *510*, 91–102. [CrossRef]
68. Rabia, M.K.; Degioanni, S.; Martinet, C.; Le Brusq, J.; Champagnon, B.; Vouagner, D. A-Thermal Elastic Behavior of Silicate Glasses. *J. Phys. Condens. Matter.* **2016**, *28*, 075402. [CrossRef]
69. Selvamani, T.; Sinhamahapatra, A.; Bhattacharjya, D.; Mukhopadhyay, I. Rectangular MgO microsheets with strong catalytic activity. *Mater Chem Phys.* **2011**, *129*, 853–861. [CrossRef]
70. Thiago Rossi, M.; Campos Juacyara, C.; Souza Mariana, M.V.M. CO_2 capture by Mg–Al and Zn–Al hydrotalcite-like compounds. *Adsorption* **2016**, *22*, 151–158. [CrossRef]
71. Kulawong, S.; Youngjan, S.; Khemthong, P.; Chanlek, N.; Wittayakun, J.; Osakoo, N. Magnesium Impregnated on NaX Zeolite Synthesized from Cogon Grass Silica for Fast Production of Fructose via Microwave-Assisted Catalytic Glucose Isomerization. *Catalysts* **2021**, *11*, 981. [CrossRef]
72. Kusumastuti, R.; Pancoko, M.; Butar-Butar, S.L.; Putra, G.E.; Tjahjono, H. Study on the mechanism of CO_2 adsorption process on zeolite 5A as a molecular sieve in RDE system: An infrared investigation. *J. Phys. Conf. Ser.* **2019**, *1198*, 032009. [CrossRef]
73. Bahmanzadegan, F.; Ghaemi, A. Modification and Functionalization of Zeolites to Improve the Efficiency of CO_2 Adsorption: A Review. *Chem. Environ. Eng.* **2024**, *9*, 100564. [CrossRef]